Ensemble simulations with discrete classical dynamics

Søren Toxvaerd[a)]
DNRF Centre "Glass and Time," IMFUFA, Department of Sciences, Roskilde University, Postbox 260, DK-4000 Roskilde, Denmark

(Received 21 June 2013; accepted 29 October 2013; published online 10 December 2013)

For discrete classical Molecular Dynamics (MD) obtained by the "Verlet" algorithm (VA) with the time increment h there exists (for sufficiently small h) a shadow Hamiltonian $\tilde{H}$ with energy $\tilde{E}(h)$, for which the discrete particle positions lie on the analytic trajectories for $\tilde{H}$. The first order estimate of $\tilde{E}(h)$ is employed to determine the relation with the corresponding energy, E, for the analytic dynamics with $h = 0$ and the zero-order estimate $E_0(h)$ of the energy for discrete dynamics, appearing in the literature for MD with VA. We derive a corresponding time reversible VA algorithm for canonical dynamics for the $(NV\tilde{T}(h))$ ensemble and determine the relations between the energies and temperatures for the different ensembles, including the $(NVE_0(h))$ and $(NVT_0(h))$ ensembles. The differences in the energies and temperatures are proportional with h^2 and they are of the order of a few tenths of a percent for a traditional value of h. The relations between $(NV\tilde{E}(h))$ and (NVE), and $(NV\tilde{T}(h))$ and (NVT) are easily determined for a given density and temperature, and allow for using larger time increments in MD. The accurate determinations of the energies are used to determine the kinetic degrees of freedom in a system of N particles. It is $3N - 3$ for a three dimensional system. The knowledge of the degrees of freedom is necessary when simulating small system, e.g., at nucleation. © *2013 AIP Publishing LLC*. [http://dx.doi.org/10.1063/1.4836615]

I. INTRODUCTION

Molecular Dynamics (MD) generates the time evolution of N classical mechanical particles by discrete time propagation. Almost all the MD are obtained by the "Verlet" algorithm (VA)[1] where a new position $\mathbf{r}_i(t+h)$ of the ith particle with mass m_i at time $t+h$ is obtained from the force $\mathbf{f}_i(t)$ and the two last discrete positions,

$$\mathbf{r}_i(t+h) = 2\mathbf{r}_i(t) - \mathbf{r}_i(t-h) + h^2\mathbf{f}_i(t)/m_i. \qquad (1)$$

The algorithm is the central-difference expression for the mass times the acceleration of the particle which equals the force $\mathbf{f}_i$, and it appears in the literature with different names (Verlet, leap-frog, velocity Verlet, etc.).[2] The algorithm is time reversible and symplectic, and the different reformulations of the algorithm do not change the discrete time evolution and the physics obtained by the VA dynamics. The algorithm deviates from all other algorithms for classical dynamics in that momenta are not dynamical variables.[3] Nevertheless, the sum of potential energy and "kinetic energy" obtained from a simple expression for the momenta reveals that the sum of potential end kinetic energy, $E_0(h)$, is constant apart from small fluctuations, and the time averages of discrete values, determined by MD with VA, are recorded as microcanonical (NVE) values for the analytic dynamics of N particles in the volume V and with the constant energy E.

Mathematical investigations[4–6] have proved the existence of a shadow Hamiltonian $\tilde{H}$[7] for symplectic algorithms. The proof is obtained by an asymptotic expansion but the series for the shadow Hamiltonian does not converge in the general case. For a review of the asymptotic expansion, its convergence and optimal truncation, see Ref. 8. If the expansion is suitably truncated, the resulting modified equations have a solution which is remarkably close to the discrete solution.[9] Only the harmonic approximation, $E_1(h)$, of the first term in this expansion is known explicitly.[2,7] Inclusion of $E_1(h)$ in the traditional obtained zero order energy, E_0, for MD systems with Lennard-Jones (LJ) particles reduces, however, the fluctuation in the energy by a factor of 100 for traditional values of h^2 and makes it possible to obtain the energy with high precision. The energy $E_0 + h^2E_1(h)$ is here presented as the first order estimate of the shadow energy

$$\tilde{E} \simeq E_0 + h^2E_1(h) + \mathcal{O}(h^4). \qquad (2)$$

So the recorded microcanonical values in the literature for MD with VA are $(NVE_0(h))$ values, presented as (NVE) values and for discrete dynamics with $(NV\tilde{E}(h))$ properties.

Here we determine the energies E, E_0, and $E_0 + h^2E_1(h)$ for a MD systems with LJ particles, obtained by the VA algorithm. For a general review of the asymptotic expansion, the shadow Hamiltonian, proofs of properties, etc., see Ref. 8.

The VA algorithm has been modified to simulate the canonical (NVT_0) ensemble,[10] where T_0 is the temperature obtained from the simple (zero-order) expression for the momenta. Here we derive a time reversible (Nosé-Hoover (NH)) VA algorithm for (NVT_0) and $(NV\tilde{T})$ simulations. The accurate dynamics for the $(NV\tilde{E})$ and $(NV\tilde{T})$ dynamics allows for a determination of the degrees of freedom in a three dimensional system of N particles and to determine the corresponding differences in energies between the $(NV\tilde{T})$ dynamics, the (NVT) dynamics, and the zero order (NVT_0) dynamics.

a)st@ruc.dk

II. THE *NVẼ* ENSEMBLE

The shadow energy $\tilde{E}$ is a function of the discrete time increment h. The harmonic approximation of the first term in the asymptotic expansion gives (Eq. (20) in Ref. 7)

$$\tilde{E}(t_n) \simeq U(\mathbf{r}(t_n)^N) + \frac{1}{2}\sum_i^N \frac{\mathbf{v}_i(t_n)^2}{1 - h^2\omega_i(t_n)^2/4} - \sum_i^N h^2 A_i(t_n)^2 \omega_i(t_n)^4/24 + \mathcal{O}(h^4), \tag{3}$$

which also can be written as[2,11,13]

$$\tilde{E}(t_n) = U(\mathbf{r}(t_n)^N) + \frac{1}{2}\sum_i^N \mathbf{v}_i(t_n)^2 + \frac{h^2}{12}\sum_i^N \left[\mathbf{v}_i(t_n)^2\omega_i(t_n)^2 - \frac{1}{2}\mathbf{f}_i(t_n)^2\right] + \mathcal{O}(h^4) \tag{4}$$

$$= U(\mathbf{r}(t_n)^N) + \frac{1}{2}\sum_i^N \mathbf{v}_i(t_n)^2 + \frac{h^2}{12}\left(\mathbf{v}_n^N\right)^T \mathbf{J}\left(\mathbf{r}_n^N\right)\left(\mathbf{v}_n^N\right) - \frac{h^2}{24}\mathbf{f}_n^N\left(\mathbf{r}_n^N\right)^2 + \mathcal{O}(h^4). \tag{5}$$

The velocities in Eqs. (3)–(5) are given by the central-difference expression

$$\mathbf{v}_i(t_n) = \frac{\mathbf{r}_i(t_n + h) - \mathbf{r}_i(t_n - h)}{2h}, \tag{6}$$

with the notations $\mathbf{v}_n^N \equiv \mathbf{v}_1(t_n), \ldots, \mathbf{v}_N(t_n)$, $\mathbf{f}_n^N \equiv \mathbf{f}_1(t_n), \ldots, \mathbf{f}_N(t_n)$, and $\mathbf{r}_n^N \equiv \mathbf{r}_1(t_n), \ldots, \mathbf{r}_N(t_n)$ at time $t_n = nh$ and with the mass m included in the time unit.

The potential energy, $U(\mathbf{r}(t_n)^N)$, and the Hessian $\mathbf{J}(\mathbf{r}_n^N)$ are functions of the positions, $\mathbf{r}(t_n)^N$, of the N particles. The potential energy of the shadow Hamiltonian at time t_n is $U(\mathbf{r}(t_n)^N)$, since the positions $\mathbf{r}(t_n)^N$ are also the positions of the particles for the analytic dynamics with $\tilde{H}(t)$. The additional terms in Eqs. (3)–(5) are the kinetic energy estimate, $\tilde{K}(t_n)$ for $\tilde{H}(t)$, obtained by the VA dynamics.

The square of the harmonic frequency, $\omega_i(t_n)^2$ at t_n with amplitudes $A_i(t_n)$, for particle i can be obtained either from the Hessian matrix $\mathbf{J}(\mathbf{r}_n^N)$ of the potential energy,[2,12,13] or simply by the usual Verlet central-difference scheme as the frequency at time t_n for a harmonic oscillator which at $\mathbf{r}_i(t_n)$ moves in the plane $[\mathbf{r}_i(t_n - h), \mathbf{r}_i(t_n), \mathbf{r}_i(t_n + h)]$,[7,11]

$$\omega_i(t_n)^2 = -\frac{(\mathbf{f}_i(t_n + h) - \mathbf{f}_i(t_n - h)) \cdot \mathbf{e}_i}{|\mathbf{r}_i(t_n + h) - \mathbf{r}_i(t - h)|}, \tag{7}$$

where $\mathbf{e}_i$ is the unit vector: $\mathbf{e}_i(t_n) = (\mathbf{r}_i(t_n + h) - \mathbf{r}_i(t_n - h))/|\mathbf{r}_i(t_n + h) - \mathbf{r}_i(t_n - h)|$.

The first two terms in Eqs. (4) and (5) give the usual zero-order expression for the energy

$$E_0(t_n) = U(\mathbf{r}(t_n)^N) + \frac{1}{2}\sum_i^N \mathbf{v}_i(t_n)^2, \tag{8}$$

with the "kinetic" energy

$$K_0(t_n) = \frac{1}{2}\sum_i^N \mathbf{v}_i(t_n)^2 = \frac{3N - \beta}{2} T_0(t_n). \tag{9}$$

The zero order estimate of the mean energy $E_0 = \langle E_0(t_n)\rangle$ and temperature $T_0 = \langle T_0(t_n)\rangle$ is obtained as the mean ($\langle\rangle$) of discrete values. The reduction, β, of the degrees of freedom of the dynamics in the kinetic part of the phase space is traditionally set to $\beta = 3$, since the VA dynamics conserves the momentum of the center of mass. The data given in this section are for the "standard" MD with VA, i.e., for T_0 obtained from K_0 and with the traditional choice $\beta = 3$. In Sec. III it will be demonstrated that $\beta = 3$ for $(NV\tilde{E})$ as well as $(NV\tilde{T})$ dynamics with VA for systems with periodical boundaries. For conservative systems without periodical boundaries $\beta = 6$ (see the Appendix).

The values obtained by MD with VA are time averages of $(NV\tilde{E}(h))$ ensemble values, but recorded as $(NVE_0(h))$ values and with

$$\tilde{K}(\tilde{T}) = \langle \tilde{K}(t_n)\rangle = \frac{3N - \beta}{2}\tilde{T} \simeq \frac{3N - \beta}{2}(T_0 + h^2\Delta T_1) + \mathcal{O}(h^4), \tag{10}$$

with

$$\Delta T_1 = \left\langle \frac{1}{6(3N - \beta)}\sum_i^N \left[\mathbf{v}_i(t_n)^2\omega_i(t_n)^2 - \frac{1}{2}\mathbf{f}_i(t_n)^2\right]\right\rangle = \left\langle \frac{1}{6(3N - \beta)}\left[\left(\mathbf{v}_n^N\right)^T \mathbf{J}\left(\mathbf{r}_n^N\right)\left(\mathbf{v}_n^N\right) - \frac{1}{2}\mathbf{f}_n^N\left(\mathbf{r}_n^N\right)^2\right]\right\rangle. \tag{11}$$

We have performed a comprehensive test of the difference between (NVE_0) and $(NV\tilde{E})$ for a LJ system of $N = 2000$ particles $T_0 \approx 1$ and $\rho = 0.8$, and with the pair forces truncated and shifted at $r_c = 2.5\sigma$.[14] The state point corresponds to a liquid state point at moderate pressure, and it is a representative state point for most of published MD data. The system has been simulated for the time increments $h = h_0 \times 2^a; a \in [0:4]$ with $h_0 = 0.000625$. Figure 1 shows the distributions of normal modes in the system for $h = h_0$ (red line) and $h = h_0 \times 2^4 = 0.01$ (green line). The two distributions are almost equal. There are only marginal differences in the distributions for high frequencies (the inset) so the discrete VA algorithm explores almost the same energy function $U(\mathbf{r}^N)$ independent of the step length h within the stability limit of VA.[11]

The energies $E_0(h)$ and $\tilde{E}(h)$ do depend on h, however, because the kinetic energies $K_0(h)$ and $\tilde{K}(h)$ corresponding to the temperatures, $T_0(h)$ and $\tilde{T}(h)$, depend on h. The first order correction term, $h^2E_1(t_n)$, has two effects on the records of energy and temperature. For a traditional choice of h it reduces the variations in the energy estimate by a factor of 100, and it shifts the corrected energy and temperature by certain amount, h^2E_1 and $h^2\Delta T_1$, proportional to h^2. This shift is state dependent and increases with the density and temperature where the term $\langle \mathbf{f}_i(t_n)^2\rangle$ is big. Figure 2 shows the

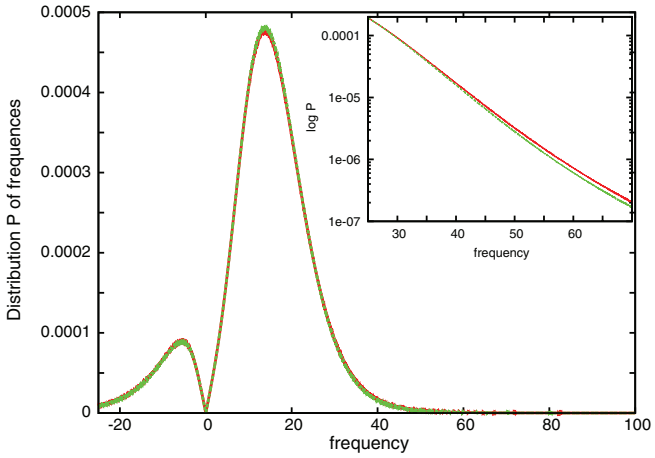

FIG. 1. Distribution, $P(\omega)$, of normal modes with frequencies ω in a LJ-fluid at $T_0 = 1$ and $\rho = 0.8$. Red lines show the distribution obtained for a small time-increment $h = 0.000625$ and with green points the distributions for $h = 0.01$. The inset shows the high frequency distributions in a $\log P(\omega)$ plot.

energies per particle $E_0(t_n)$ (red line) and $\tilde{E}(t_n)$ (green line) for a traditional choice $h = 0.005$. Inclusion of $h^2E_1(t_n)$ shifts the energy and reduces the fluctuations dramatically. The means $\langle E_1(t_n)\rangle$ and $\Delta T_1(t_n)$ are, however independent of h. The inset in Figure 2 shows $\Delta T_1(t_n)$ for $h = 0.000625$ (red line) and $h = 0.01$ (green line). Not only the mean square force, $\langle \mathbf{f}_i(t_n)^2\rangle$ and instantaneous frequency spectrum, but also $\langle \mathbf{v}_i(t_n)^2\omega_i(t_n)^2\rangle$, and thereby $\langle E_1(t_n)\rangle$ and $\Delta T_1(t_n)$ are rather independent of h.

Table I shows the determination of E_0/N and $\tilde{E}/N$ for a LJ fluid at $\rho = 0.8$ and $T_0 = 1$ (with $\beta = 3$). The data for a given value of h are obtained by interpolations from three independent sets of (NVE) MD each with 10^7 steps. The three subsets were for temperatures near $T_0 = 1$, and the values given in the table are obtained from interpolations to $T_0 = 1$ from these three values.

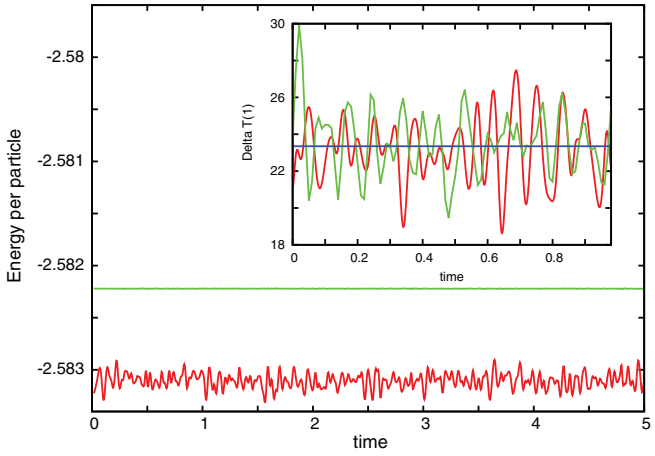

FIG. 2. Energy per particle for a LJ fluid at $\rho = 0.8$ and $T_0 = 1$ as a function of time $t = n \times h$ and for $h = 0.005$. The red line is the traditional zero order estimate $E_0(t_n)$ and the green line is $\tilde{E}(t_n) \simeq E_0(t_n) + h^2E_1(t_n)$. The inset shows ΔT_1 for $h = 0.000625$ (red line) and $h = 0.01$ (green line). The blue straight line is the mean $\langle \Delta T_1(t_n)\rangle = 23.35$, which is the same for both values of h.

TABLE I. Energies per particle of a LJ fluid at $T_0 = 1$ (with $\beta = 3$) and $\rho = 0.8$.

h	E_0/N	$\tilde{E}/N$	U/N
0	− 2.58936	− 2.58936	− 4.08852
0.000625	− 2.589426	− 2.589413	− 4.088676
0.001250	− 2.589225	− 2.589170	− 4.088474
0.002500	− 2.588898	− 2.588694	− 4.088164
0.005000	− 2.587915	− 2.587041	− 4.086731
0.010000	− 2.583507	− 2.579988	− 4.082758

The established h^2 dependence of the different energies (Figure 3) makes it uncomplicated to extrapolate to the energies for the analytic dynamics at ρ, T, e.g.,

$$\lim_{h\to 0} E_0(h, T_0) = \lim_{h\to 0} \tilde{E}(h, \tilde{T}) = E(\rho, T), \tag{12}$$

and to determine the difference between the MD time averages and the NVE ensemble values. The value for $h = 0$ in Table I represents the extrapolations to the values for $\rho = 0.80, T = 1$ for the analytic dynamics.

The traditional MD with VA records $(NVE_0(h))$ ensemble values for the exact $(NV\tilde{E}(h))$ dynamics and the values are presented as (NVE) values! The errors by these imprecise estimates are, however, rather small for traditional choices of state points and values of h. Most LJ simulations are obtained for $h = 0.005$ for which the differences between the different energy records are of the order a few tenths of a percent and of the same order as the uncertainties in pressures and free energies. The energies for $(NVE_0(h))$ and $(NV\tilde{E}(h))$ in Table I are shown in Figure 3. The data in Table I reveal that also the mean of the discrete potential energies, U/N, obtained by MD with VA at constant T_0 depends on h, and with the same dependence

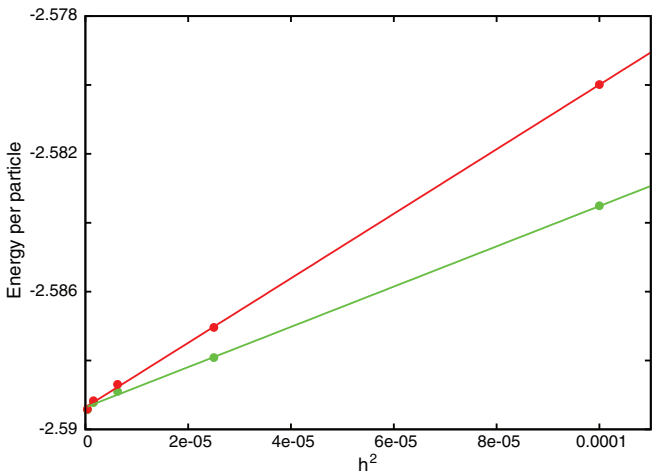

FIG. 3. Energies per particle in a LJ fluid at $\rho = 0.8$ and $T_0 = 1$ as a function of h^2. Red points are $\tilde{E}(h)/N$ and green points are $E_0(h)/N$. The lines $E/N + \alpha h^2$, where E/N is the energy for analytic dynamics, have the slope $\alpha(\tilde{E}/N) = 93.68$ and $\alpha(E_0/N) = 58.43$.

$\langle U(\mathbf{r}(t_n)^N)/N\rangle = U(T)/N + 58.36 \times h^2$ as that of $E_0(h)/N$ (because $\langle K_0/N\rangle$ is fixed by $T_0 = 1$).

III. THE $NV\tilde{T}$ ENSEMBLE

The thermodynamic temperature T can be obtained not only from the mean of momenta in the phase space, but also as a mean obtained from the configurational part of the phase space.[15] Although the temperature traditionally is obtained by MD from the mean kinetic energy $K_0(T_0)$, it can equally be well obtained from the energy function $U(\mathbf{r}^N)$, e.g., as[16]

$$T_{\rm conf} = \frac{\left\langle \sum_i^N \mathbf{f}_i(t_n)^2 \right\rangle}{-\left\langle \sum_i^N \nabla \cdot \mathbf{f}_i(t_n) \right\rangle}, \tag{13}$$

where the ensemble average in MD is replaced by averages over the discrete time values. (The configurational temperature $T_{\rm conf}$ is given by different expressions,[16] which however, are equal in the thermodynamic limit $N \simeq \infty$.) Since the dynamics with VA takes place in the configurational part of the phase space it is perhaps more natural to obtain the temperature as $T = T_{\rm conf}$, than obtaining it from an approximate expression for the kinetic energy. The question is what relation there is between the thermodynamic temperature T for analytic dynamics, the configurational temperature $T_{\rm conf}(h)$, and the temperatures $T_0(h)$ and $\tilde{T}(h)$ for discrete canonical dynamics with the VA algorithm.

A. The Nosé-Hoover thermostat

The mean values of MD with VA for the (NVT) ensemble can be obtained by Nosé-Hoover dynamics.[17,18] The NH dynamics adds a friction term, η, to the forces. In the Hamilton formulation of classical mechanics the dynamic equations are

$$\dot{\mathbf{r}}_i(t) = \mathbf{p}_i(t), \tag{14}$$

$$\dot{\mathbf{p}}_i(t) = \mathbf{f}_i(t)/m_i - \eta(t)\mathbf{p}_i(t), \tag{15}$$

$$\dot{\eta}(t) = \alpha^{-1}(K(t) - K(T)), \tag{16}$$

with a restoring friction force $\eta(t)$ which "constrains" the kinetic energy $K(t)$ to the energy $K(T) = \frac{(3N-\beta)}{2}T$. The damping factor α is expressed as[21]

$$\alpha = (3N - \beta)T\tau^2, \tag{17}$$

where β usually is set to $\beta = 3$ in MD with conserved momentum of the center of mass, and $\tau > h$ is a characteristic oscillation time of the thermostat. We shall determine the value of β in Sec. III C. The constrained dynamics generates canonical phase-space distributions, although it is not Hamiltonian dynamics. The dynamics is not symplectic, but in mean it conserves the phase space density, and it has an energy-like constant of motion.[19] The theoretical foundation is given, e.g., in Refs. 10 and 17–19, here we concentrate on its implementation for discrete dynamics with the VA algorithm.

B. A Verlet algorithm for (NVT_0) and $(NV\tilde{T})$ dynamics

It is most convenient to formulate constant temperature dynamics by the "leap frog" formulation of VA, which corresponds to the discretisation of Hamilton's equations for classical dynamics, although the momenta are not dynamical variables in the VA dynamics. In the leap-frog formulation of VA dynamics one introduces the variables for the "velocities" in the time interval $t \in [t_n - h, t_n] : \mathbf{v}_i(t_n - h/2) \equiv (\mathbf{r}_i(t_n) - \mathbf{r}_i(t_n - h))/h$. With this notation the VA velocities, in $K_0(t_n)$ and $\tilde{K}(t_n)$, are

$$\mathbf{v}_i(t_n) = \frac{\mathbf{v}_i(t_n + h/2) + \mathbf{v}_i(t_n - h/2)}{2}. \tag{18}$$

Time reversible discrete algorithms for(NVT_0) dynamics have appeared in the literature for several decades,[20–23] and they differ a little from the algorithm derived here. Three of them (Refs. 20–22) use

$$K_{1/2}(t_n + h/2) = \frac{1}{2}\sum_i^N \mathbf{v}_i(t_n + h/2)^2 \tag{19}$$

for the kinetic energy in the dynamics of the thermostat equation (16), and this approximation introduces an unnecessary imprecision of the temperature T_0. It is easy to derive the following relation:

$$\mathbf{v}_i(t_n)^2 = \frac{1}{2}\mathbf{v}_i(t_n + h/2)^2 + \frac{1}{2}\mathbf{v}_i(t_n - h/2)^2 - \frac{1}{4}h^2\mathbf{f}_i(t_n)^2 \tag{20}$$

for the VA algorithm. This means that the zero order expression, Eq. (9), for the kinetic energy $K_0(t_n)$ can be written as

$$K_0(t_n) = \frac{1}{2}\left[K_{1/2}(t_n + h/2) - \frac{1}{8}h^2\sum_{i=1}^N \mathbf{f}_i(t_n)^2\right] + \frac{1}{2}\left[K_{1/2}(t_n - h/2) - \frac{1}{8}h^2\sum_{i=1}^N \mathbf{f}_i(t_n)^2\right] \tag{21}$$

and with the consequence that

$$K_0(T_0) = \langle K_{1/2}(t_n + h/2) - \frac{1}{8}h^2\sum_{i=1}^N \mathbf{f}_i(t_n)^2\rangle \equiv K_{1/2}(T_0). \tag{22}$$

The term $\langle -\frac{1}{8}h^2\sum_{i=1}^N \mathbf{f}_i(t_n)^2\rangle$ was not included in the thermostats[20–22] and this omission gives, in a systematic way, an error in the thermostat temperature T_0. The error is proportional to h^2 and of the order of a few tenths of a percent at $\rho = 0.80$ for a traditional choice of time increment. (The error is, however, significantly larger at higher densities.)

The dynamics of the friction can be determined either by[20–22]

$$\dot{\eta}(t_n) = \frac{\eta(t_n + h) - \eta(t_n)}{h} = \alpha^{-1}\Delta K(t_n), \tag{23}$$

and using $\Delta K(t_n) = K_{1/2}(t_n + h/2) - \frac{1}{8}h^2\mathbf{f}_i(t_n)^2 - K_{1/2}(T_0)$ in the time interval $[t_n, t_n + h]$ in a (NVT_0) and $\Delta K(t_n) = \tilde{K}(t_n) - \tilde{K}(\tilde{T})$ in a $(NV\tilde{T})$ simulation, or the dynamics of η can be obtained by a central-difference expression at

time t_n:[23]

$$\dot{\eta}(t_n) = \frac{\eta(t_n + h) - \eta(t_n - h)}{2h} = \alpha^{-1}\Delta K(t_n), \tag{24}$$

with $\Delta K(t_n) = K_0(t_n) - K_0(T_0)$ for (NVT_0) in the time interval $[t_n - h, t_n + h]$ and $\Delta K(t_n) = \tilde{K}(t_n) - \tilde{K}(\tilde{T})$ for $(NV\tilde{T})$.

The position $\mathbf{r}_i(t_n + h)$ for a particle i is generated from two sets of positions $\mathbf{r}_i(t_n)$ and $\mathbf{r}_i(t_n - h)$, and friction(s) $\eta(t_n)$ and $\eta(t_n - h)$ for Eq. (24). A loop with VA discrete dynamics is started with calculation of the forces $\mathbf{f}(t_n)^N$ at time t_n from the positions $\mathbf{r}(t_n)^N$. In the next step the leap-frog velocities are updated to time $t_n + h/2$. The central difference implementation of Eq. (14) is (masses included in the time unit)

$$\frac{\mathbf{v}_i(t_n + h/2) - \mathbf{v}_i(t_n - h/2)}{h} = \mathbf{f}_i(t) - \eta(t_n)\frac{\mathbf{v}_i(t_n + h/2) + \mathbf{v}_i(t_n - h/2)}{2}, \tag{25}$$

which implies

$$\mathbf{v}_i(t_n + h/2) = \frac{h\mathbf{f}_i(t_n) + \mathbf{v}_i(t_n - h/2)\left(1 - h\frac{\eta(t_n)}{2}\right)}{1 + h\frac{\eta(t_n)}{2}}, \tag{26}$$

and the leap-frog velocity is updated to $\mathbf{v}_i(t_n + h/2)$ by using $\mathbf{v}_i(t_n - h/2)$, $\mathbf{f}_i(t_n)$ and $\eta(t_n)$. The new positions at $t_n + h$ are updated by

$$\mathbf{r}_i(t_n + h) = \mathbf{r}_i(t_n) + h\mathbf{v}_i(t_n + h/2), \tag{27}$$

and then the new value, $\eta(t_n + h)$, is obtained by either

$$\eta(t_n + h) = \eta(t_n) + h\alpha^{-1}\Delta K(t_n) \tag{28}$$

for the NHVA with Eq. (23) for the dynamics of the friction, or by

$$\eta(t_n + h) = \eta(t_n - h) + 2h\alpha^{-1}\Delta K(t_n) \tag{29}$$

for NHVA with Eq. (24).

The kinetic energy $K_0(t_n)$ can be calculated directly for the simple (NVT_0), but the expressions, Eqs. (10) and (11), for the kinetic energy, $\tilde{K}(t_n)$, of the shadow Hamiltonian depend implicitly on the "velocities" $\mathbf{v}_i(t_n + h/2)$. This apparent complication is, however, easily overcome by postponing the updating of the friction at t_n to after the updating of $\mathbf{v}_i(t_n + h/2)$, as described above, and using Eq. (5) to obtain the kinetic energy $\tilde{K}(t_n)$.

Although the (NVT_0) and $(NV\tilde{T})$ algorithms sample discrete canonical distributed values, the momenta have no impact on the dynamics, and the algorithms can also be presented as Verlet algorithms for discrete dynamics. By eliminating the momenta one obtains the algorithm (NHVA), for discrete canonical dynamics,

$$\mathbf{r}_i(t_n + h) = \frac{2\mathbf{r}_i(t_n) + h^2\mathbf{f}_i(t_n) - \mathbf{r}_i(t_n - h)\left(1 - h\frac{\eta(t_n)}{2}\right)}{1 + h\frac{\eta(t_n)}{2}}, \tag{30}$$

and with the dynamics of the friction obtained either from Eq. (23) or Eq. (24).

The VA and NHVA dynamics and the shadow energy are determined with only two sets of start positions (and friction(s)) and the time increment. The NHVA is not symplectic, but at a given time t_n and with the two sets of positions, $\mathbf{r}(t_n)^N$ and $\mathbf{r}(t_{n-1})^N$, there is a shadow Hamiltonian for the $(NV\tilde{E})$ dynamics and with the energy $\tilde{E}(n) = U(t_n) + \tilde{K}(t_n)$ with a mean $(NV\tilde{E})$ potential energy $U(n)$ and kinetic energy $\tilde{K}(n)$. The next step can be taken either with VA dynamics without a "temperature" adjustment and thus with this shadow energy, or one can obtain the NHVA positions by Eq. (30). But since this NHVA step is not symplectic the shadow energy, $\tilde{E}(n+1)$, for the discrete sets of points, $\mathbf{r}(t_{n+1})^N$, $\mathbf{r}(t_n)^N$ with $\mathbf{r}(t_{n+1})^N$ obtained by NHVA differs from $\tilde{E}(n)$. The NHVA dynamics conserves the phase space (mean) density and the obtained NHVA energy must be the mean $\langle\tilde{E}(n)\rangle$ of the shadow energies for consecutive sets of positions.

The change in the friction is obtained from the excess shadow kinetic energy $\Delta K(t_n)$, but since the dynamics is in the configurational part of the phase space the question is whether the excess of the shadow kinetic energy $\Delta K(t_n)$ could be replaced by the excess of potential energy $\Delta U(t_n)$. The NHVA dynamics is started from two sets of positions, $\mathbf{r}(t_1)^N$ and $\mathbf{r}(t_0)^N$, which have a shadow energy $\tilde{E}(1) = U(t_1) + \tilde{K}(t_1)$. For the nth NHVA step and with $\tilde{K}(\tilde{T}) = \tilde{K}(t_1)$,

$$\Delta K(t_n) = \tilde{K}(t_n) - \tilde{K}(t_1) = \tilde{E}(n) - U(t_n) - (\tilde{E}(1) - U(t_1)) = \Delta\tilde{E}(t_n) + \Delta U(t_n) \approx \Delta U(t_n), \tag{31}$$

with $\Delta U(t_n) = U(t_1) - U(t_n)$ and where $\Delta\tilde{E}(t_n) = \tilde{E}(n) - \tilde{E}(1) \ll \Delta U(t_n)$ and $\langle\Delta\tilde{E}\rangle = 0$. The velocities are Gaussian distributed, but the potential energies of the particles are not. The NH dynamics maintain the Gaussian distribution of the velocities, but the non-Gaussian distribution of the potential energies of the N particles implies that, although the dynamics only take place in the configurational part of the phase space one cannot directly use the excess potential energy in the equation for the dynamics of the friction. A configurational NH thermostat is obtained by using the expression(s) for the configurational temperature.[24,25]

C. Results

The $(NV\tilde{T})$ dynamics has been performed for the LJ-fluid at $\rho = 0.80$ and $\tilde{T} = 1$, for different values of the time increment h and for shifted LJ-forces (SF) and shifted LJ-potentials (SP). The question is what relation there is between the exact VA dynamics with the $(NV\tilde{E}(h))$ properties and the NHVA, which only is symplectic in mean. A related question is how many degrees of freedom there are for the two ensemble dynamics. The high precision energy data allow for a determination of β, and we have started the investigation by determining the degrees of freedom, β, for the two ensembles. Since the $(NV\tilde{E}(h))$ dynamics is for an unknown $\tilde{H}(t)$, it is not obvious what role a conservation of the center of mass and its momentum by the discrete VA time propagation in the configurational part of the phase space plays for the residual kinetic energy of an unknown Hamiltonian. For the canonical dynamics the situation is even more unclear. The $(NV\tilde{T})$ dynamics is only symplectic in mean, but contains a conserved

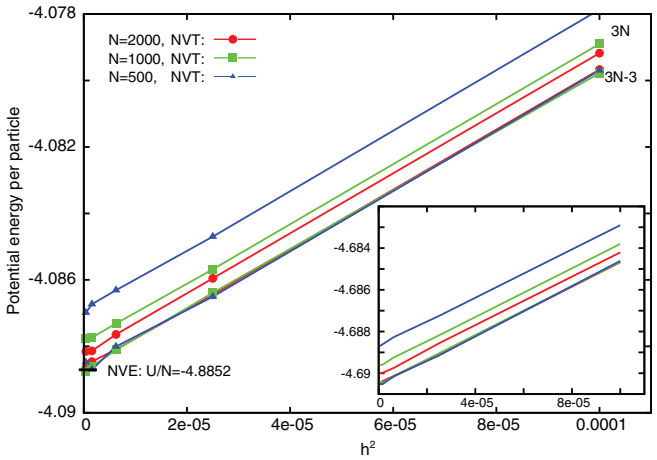

FIG. 4. The $(N\,V\,\tilde{T})$ potential energies per particle obtained by the NHVA for a LJ SF system at $\rho = 0.80$ and $\tilde{T} = 1$. Red line and filled circles are for $N = 2000$. Green line and filled squares are for $N = 1000$, and blue lines and filled triangles are for $N = 500$. The kinetic part of the shadow Hamiltonian, $\tilde{K}$, is constrained in two sets of data; in the upper set to $3N$ degrees of freedom and in the lower set of data to $3N - 3$ degrees of freedom. The black line at the ordinate axis is $U/N = -4.08852$ for $(N\,V\,E)$ dynamics from Table I. The inset shows the corresponding result for $(N\,V\,\tilde{T}_0)$ dynamics for a LJ SP system (traditional NHVA dynamics).

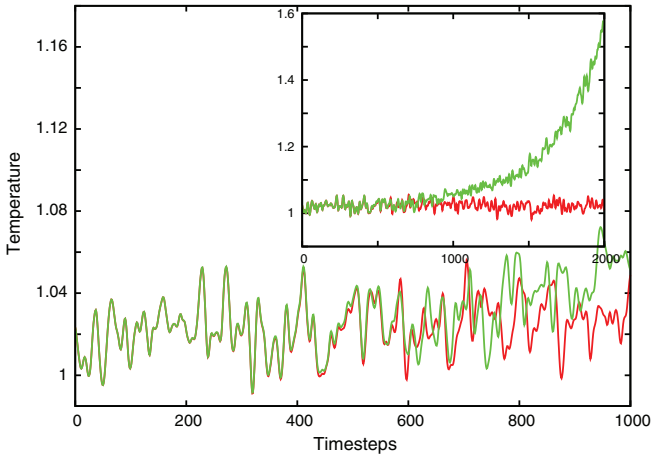

FIG. 5. Instant temperatures as a function of time steps with $(N\,V\,\tilde{T})$ dynamics. Red line is with traditional expression $\Delta K(t_n) = \tilde{K}(t_n) - K(t_1)$; green line is for $\Delta\tilde{K}(t_n) = U(t_1) - U(t_n)$. The inset includes the next 1000 time steps.

energy-like bond.[19] If the momentum of the center of mass is set to zero at the start of the NHVA dynamics, the location of the center of mass and its momentum is conserved accordingly to Eq. (30) (see the Appendix).

The simulations have been performed for LJ systems with $N = 500$, 1000, and 2000 particles and for $(N\,V\,\tilde{E}(h))$, $(N\,V\,\tilde{T}(h))$, and $(N\,V\,T_0)$ dynamics in order to determine the number, β of degrees of freedom for the discrete dynamics. The systems are simulated with the NHVA algorithm for the temperature equal to one and with the kinetic part, $\tilde{K}(\tilde{T}) = \frac{3N-\beta}{2}$. The three systems have identical mean particle distributions, given by the radial distribution function $g(r)$ at the same density and temperature, so the system sizes are large enough that intensive bulk properties, such as the potential energy per particle should be the same for the three systems at a given (T, ρ) state point. Figure 4 shows the mean potential energy per particle $U(h)/N$ for 10^7 time steps per simulation, obtained by the NHVA algorithm for the three system sizes and for two sets of degrees of freedom, $\beta = 0$ and $\beta = 3$. If the potential energy per particle is independent of N for $\beta = 0$, it corresponds that the conservation of the center of mass and its momentum has no impact on the dynamics, while $\beta = 3$ accounts for the constraint on the momentum of the center of mass; this value is probably used for most MD data in the literature. The three sets of $(N\,V\,\tilde{T}(h))$ energies per particle agree only for $\beta = 3$. The black line at the ordinate axis in the figure is the U/N value for $(N\,V\,E)$ dynamics from Table I for $3N - 3$ degrees of freedom and for analytic dynamics for $h = 0$. The sensitivity of this result with respect to the accuracy of the thermostating and the treatment of the force field was investigated by repeating the simulation for $(N\,V\,T_0(h))$ dynamics and with truncated and shifted potentials (traditional NHVA dynamics). The inset in Figure 4 shows the corresponding data for the NHVA $(N\,V\,T_0(h))$ dynamics for the LJ SP systems. This traditional NHVA dynamics behaves qualitatively in the same manner as $(N\,V\,\tilde{T}(h))$ SF-dynamics and with the potential energy density independent of N for $3N - 3$ kinetic energy degrees of freedom. Also, the potential energy $U(h)/N$ for $(N\,V\,\tilde{E})$ and for different system sizes behaves qualitatively as $U(h)/N$ for $(N\,V\,\tilde{T})$ and has only size-independent potential energies per particle for $\beta = 3$. The angular momenta for the uniform systems with periodical boundaries are not conserved and during the very long simulations the three kinetic degrees of freedom for the angular momenta are calibrated. For conservative systems without periodical boundaries (e.g., droplets) the kinetic degrees of freedom for NHVA are $3N - 6$ (see the Appendix).

The equivalence between the usual formulation of the NH thermostat with the change in the friction proportional to the excess kinetic energy and the alternative expressions, Eq. (31), where the change in the friction is obtained directly from the change in the instant potential energy, is shown in Figure 5. The MD is started from the same sets of positions, $\mathbf{r}(t_1)^N$ and $\mathbf{r}(t_0)^N$. The excess kinetic energy for $\Delta K(t_n) = \tilde{K}(t_n) - \tilde{K}(t_1)$ has been used in the first case (red line), whereas we have used the alternative expression $\Delta K(t_n) = U(t_1) - U(t_n)$ (green line) in the second case. The figure shows the first 1000 time steps and the inset also includes the next 1000 steps. The temperatures of the two thermostats at the onset of the dynamics are equal; but the particles' potential energies at t_n are not Gaussian distributed and the scaling by using the excess potential energy destroys the conservation of the mean energy in the system. Whether the temperature $\tilde{T}$ in NHVA dynamics in fact is the configurational temperature or a temperature for the shadow momenta part of the phase space cannot be determined uniquely in this way.

The differences between the zero-order temperature T_0 obtained from $K_0(T_0)$, and $\tilde{T}$ obtained from $\tilde{K}(\tilde{T})$ are of the order of a few tenths of a percent for traditional LJ state points and time increments. The differences are shown (red line and points) in Figure 6 for the LJ fluid with density $\rho = 0.80$ and temperature $\tilde{T} = 1$. Also shown in the figure with green line

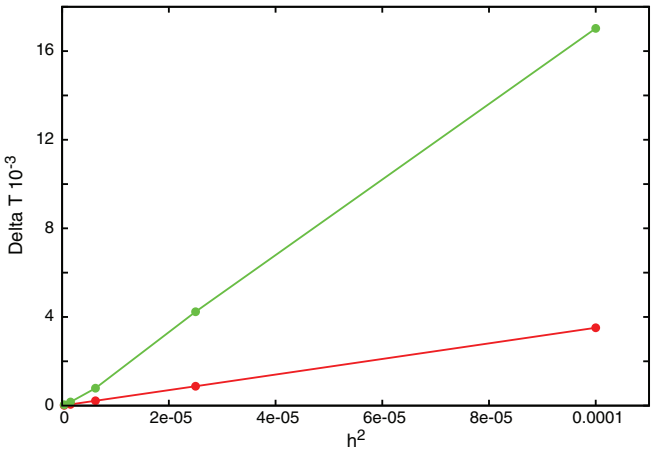

FIG. 6. Temperature difference $\Delta T = (T - \tilde{T}) \times 10^3$ for the LJ fluid at $\tilde{T} = 1$ as a function of the square h^2 of the time increment. Red line and points are the difference $T_0 - \tilde{T}$ between the traditional temperature T_0 and the shadow temperature $\tilde{T}$. Green line and points are the difference between the configurational temperature $T_{\rm conf}$ and $\tilde{T}$.

and points are the corresponding differences between the configurational temperature $T_{\rm conf}$ and $\tilde{T} = 1$. There are small and systematic differences between T_0, $T_{\rm conf}$, and $\tilde{T}$ proportional with h^2 of the order of a few tenths of a percent for a traditional time increment, and the differences go to zero in the limit of small time increments. The differences depend, however (through the term proportional to $h^2/24 \sum \mathbf{f}_n^N$ in Eq. (5)) on the pressure and the time-increment and they are significant for large pressures and time-increments.

IV. CONCLUSIONS

Molecular dynamics with the discrete VA is exact in the sense that for sufficient small time increments there exists a shadow Hamiltonian $\tilde{H}$ for which the discrete points lie on the analytic trajectories of $\tilde{H}$. MD with VA represents time averages for the microcanonical ensemble $(NV\tilde{E})$ by this Hamiltonian. The energies reported in traditional MD with VA are the zero-order estimates $E_0(h)$ of the shadow energy $\tilde{E}$ for the $(NV\tilde{E})$ ensemble, but they are presented as the energies for analytic dynamics for the (NVE) ensemble, obtained by analytic dynamics with $h = 0$. The differences between E, $E_0(h)$, and $\tilde{E}(h)$ are functions of the time increment h and for condensed systems at high densities and temperature, these differences are not negligible. To first order in the asymptotic expansion the differences are proportional to h^2, and it is easy to determine the (harmonic) correction terms. This fact allows for the use of larger time increments in MD without loss of accuracy.

It is possible to extend the VA dynamics to simulate the corresponding canonical $(NV\tilde{T}(h))$ ensemble, where the discrete dynamics are constrained to the kinetic energy of $\tilde{H}(h)$. MD simulations with this algorithm are used to determine the degrees of freedom in a system of N Lennard-Jones particles. The number is $3N - 3$ for $(NV\tilde{T})$ as well as for $(NV\tilde{E})$ simulations. For dynamics of small systems (e.g., droplets) a correct reduction of degrees of freedom is important (see the Appendix). The energies $\tilde{E}(\tilde{T})$ deviate from $E(\tilde{T} = T)$ proportional to h^2 and, as for the microcanonical simulations, it is easy to establish the dependence for a given density and temperature.

The momenta are not dynamic variables in VA dynamics, and they have no impact on the dynamics. The kinetic energies and the temperatures are obtained from the difference between the shadow energies and the potential energies U, and for the recorded MD data in the literature as the difference between the zero-order estimate $E_0(T_0)$ and U. Despite the fact that the dynamics alone depends on properties in the configurational part of the phase space, the temperature $\tilde{T}$ as well as zero-order estimate T_0 deviates, from the configurational temperature $T_{\rm conf}$ obtained directly from U.[16] The systematic differences are however small and negligible for a traditional choice of h.

The Nosé-Hoover thermostat is given by Eq. (23) or Eq. (24) together with Eqs. (26) and (27) (leap-frog) or alternatively by Eq. (30) (Verlet). The temperature to zero order in the asymptotic expansion, T_0, is obtained by Eq. (9), or if one uses Eq. (19) for the instant kinetic energy, by Eq. (22). There is only a marginal computational overhead by calculating the kinetic energy and the temperature T_0 because it is a few arithmetic operations proportional to the number of particles N. To first order in the asymptotic expansion the temperature contains an additional term given by Eq. (11). This term depends on Hessian matrix $\mathbf{J}(\mathbf{r}^N)$ and the number of arithmetic operations is proportional to N^2, but the contribution to the term can be sampled directly during the calculations of the forces and with a computational overhead of computer time only of the order of some percents depending on N. (For LJ interactions the necessary formulae are given in Appendix A of Ref. 2 and it is easy to derive the corresponding expressions for other pair interactions.)

The main investigation has been performed for systems of Lennard-Jones particles in a condensed fluid at the density $\rho = 0.8$ and temperature(s) $T = 1$. This state point is representative for most MD data with VA dynamics reported in the literature. The differences between the different ensembles, which are proportional to h^2, are small for traditional choice of densities, temperature, and time-increment. But for high densities, temperatures, and large time increments one needs to take these differences into account.

ACKNOWLEDGMENTS

The author acknowledges useful discussions with Ole J. Heilmann. The centre for viscous liquid dynamics "Glass and Time" is sponsored by the Danish National Research Foundation (DNRF) Grant No. DNRF61.

APPENDIX: NHVA DYNAMICS

The discrete Verlet algorithm for Nosé-Hoover dynamics (NHVA) with conservative forces maintains the location of the center of mass $\mathbf{R}$, its momentum, and the angular momentum $\mathbf{L}$ provided that the momentum and angular momentum are zero at the start of the simulation. With the notation $\alpha_n \equiv h\frac{\eta(t_n)}{2}$ and by subtraction of $\mathbf{r}_i(t_n)(1 + \alpha_n)$ from Eq. (30)

for the new position $\mathbf{r}_i(t_n + h)$ of particle i, one obtains

$$(\mathbf{r}_i(t_n + h) - \mathbf{r}_i(t_n))(1 + \alpha_n) = 2\mathbf{r}_i(t_n) + h^2\mathbf{f}_i(t_n) - \mathbf{r}_i(t_n - h)(1 - \alpha_n) - \mathbf{r}_i(t_n)(1 + \alpha_n). \quad \text{(A1)}$$

With the notation $\mathbf{r}_n^N$ for the positions of all the N particles at time t_n one gets

$$\left(\mathbf{r}_{n+1}^N - \mathbf{r}_n^N\right)(1 + \alpha_n) = 2\mathbf{r}_n^N - \mathbf{r}_{n-1}^N(1 - \alpha_n) - \mathbf{r}_n^N(1 + \alpha_n), \quad \text{(A2)}$$

because the sum over forces is zero for the conservative system. By a rearrangement of Eq. (A2) one obtains

$$\mathbf{r}_{n+1}^N - \mathbf{r}_n^N = \left(\mathbf{r}_n^N - \mathbf{r}_{n-1}^N\right)(1 - \alpha_n)/(1 + \alpha_n) \quad \text{(A3)}$$

so the center of mass is constant and its momentum is zero for NHVA dynamics with $(\mathbf{r}_0^N - \mathbf{r}_{-1}^N) = 0$ at the start of a constant temperature simulation.

The conservation of the angular momentum $\mathbf{L}$ for a conservative dynamics can be derived in a similar way. Consider the quantity defined by

$$2h\mathbf{L}_n \equiv \mathbf{r}_n^N \times \left(\mathbf{r}_{n+1}^N - \mathbf{r}_{n-1}^N\right). \quad \text{(A4)}$$

Inserting Eq. (30) in Eq. (A4) gives

$$2h\mathbf{L}_n(1 + \alpha_n) = \mathbf{r}_n^N \times \left(2\mathbf{r}_n^N - \mathbf{r}_{n-1}^N(1 - \alpha_n) - \mathbf{r}_{n-1}^N(1 + \alpha_n)\right) + h^2\mathbf{r}_n^N \times \mathbf{f}_n^N. \quad \text{(A5)}$$

The last term is a sum over ij terms $\mathbf{r}_i \times \mathbf{f}_{ij}$, and it cancels because

$$\mathbf{r}_i \times \mathbf{f}_{ij} + \mathbf{r}_j \times \mathbf{f}_{ji} = (\mathbf{r}_i - \mathbf{r}_j) \times \mathbf{f}_{ij} = 0 \quad \text{(A6)}$$

for central forces.

The first term in Eq. (A5) is equal to

$$2h\mathbf{L}_n(1 + \alpha_n) = \mathbf{r}_{n-1}^N \times 2\mathbf{r}_n^N, \quad \text{(A7)}$$

and if the momentum of the center of mass is zero one obtains

$$\begin{aligned} 2h\mathbf{L}_n(1 + \alpha_n) &= \mathbf{r}_{n-1}^N \times \left(2\mathbf{r}_n^N - \left(\mathbf{r}_n^N - \mathbf{r}_{n-1}^N\right) + \left(\mathbf{r}_{n-1}^N - \mathbf{r}_{n-2}^N\right)\right) \\ &= \mathbf{r}_{n-1}^N \times \left(\mathbf{r}_n^N - \mathbf{r}_{n-2}^N\right) = 2h\mathbf{L}_{n-1}. \end{aligned} \quad \text{(A8)}$$

So the angular momentum is zero with NHVA dynamics if the momentum and the angular momentum are zero at the start of the simulation.

The periodical boundaries do not destroy the conservation of the momentum, but they destroy the conservation of the angular momentum because Eq. (A6) is not valid when a particle j moves away from particle i and is replaced with a new image with a new direction of the force $\mathbf{f}_{ij}$. Thus the kinetic degrees of freedom is $3N - 3$ and not $3N - 6$ for systems with periodical boundaries. But for a (small) droplet, e.g., surrounded by gas particles a new "problem" arises. If, on one hand, it is simulated as a conservative system without periodical boundaries, the kinetic degrees of freedom is $3N - 6$. But the system is not an equilibrium system, and although the vapor pressure might be very small, the droplet will slowly evaporate. If one on the other hand applies an external field, i.e., a closed system,[26] or if one uses periodical boundaries the kinetic degrees of freedom is $3N - 3$, but the calibration of the angular momentum's three degrees of freedom is extremely slow. In practice one could set the momentum and the angular momentum to zero at the start of the simulation with NHVA with $3N - 6$ kinetic degrees of freedom, and reset the momentum and the angular momentum to zero every time a gas particle is reflected at a wall, or if a new image of the gas particle is used.

[1] L. Verlet, Phys. Rev. **159**, 98 (1967).
[2] S. Toxvaerd, O. J. Heilmann, and J. C. Dyre, J. Chem. Phys. **136**, 224106 (2012).
[3] T. D. Lee, J. Stat. Phys. **46**, 843 (1987).
[4] J. M. Sanz-Serna, Acta Numerica **1**, 243 (1992).
[5] E. Hairer, Ann. Numer. Math. **1**, 107 (1994).
[6] S. Reich, SIAM J. Numer. Anal. **36**, 1549 (1999).
[7] S. Toxvaerd, Phys Rev. E **50**, 2271 (1994). (The word *shadow Hamiltonian* was introduced in this paper, inspired by the terms *a slightly perturbed Hamiltonian* [H. Yoshida, Phys. Lett. A **150**, 262 (1990)] and *shadow trajectories* [C. Grebogi, S. M. Hammel, J. A. Yorke, and T. Saur, Phys. Rev. Lett. **65**, 1527 (1990)]).
[8] E. Hairer, C. Lubich, and G. Wanner, *Geometrical Numerical Integration* (Springer Books Archives, 2006).
[9] R. D. Skeel and D. J. Hardy, SIAM J. Sci. Comput. **23**, 1172 (2001); R. D. Skeel, *ibid.* **31**, 1363 (2009).
[10] M. P. Allen and D. J. Tildesley, *Computer Simulation of Liquids* (Oxford Science Publications, Oxford, 1987); D. Frenkel and B. Smit, *Understanding Molecular Simulation* (Academic, New York, 2002).
[11] S. Toxvaerd, J. Chem. Phys. **137**, 214102 (2012).
[12] G. Seeley and T. Keyes, J. Chem. Phys. **91**, 5581 (1989).
[13] J. Gans and D. Shalloway, Phys. Rev. E **61**, 4587 (2000).
[14] S. Toxvaerd and J. C. Dyre, J. Chem. Phys. **134**, 081102 (2011).
[15] H. H. Rugh, Phys. Rev. Lett. **78**, 772 (1997).
[16] O. G. Jepps, G. Ayton, and D. E. Evans, Phys. Rev. E **62**, 4757 (2000).
[17] S. Nosé, Mol. Phys. **52**, 255 (1984).
[18] W. G. Hoover, Phys. Rev. A **31**, 1695 (1985).
[19] H. Posch, W. G. Hoover, and F. J. Vesely, Phys. Rev. A **33**, 4253 (1986).
[20] S. Toxvaerd, Mol. Phys. **72**, 159 (1991).
[21] D. J. Evans and B. L. Holian, J. Chem. Phys. **83**, 4069 (1985).
[22] B. L. Holian, A. J. De Groot, W. G. Hoover, and C. G. Hoover, Phys. Rev. A **41**, 4552 (1990).
[23] M. Tuckerman, B. J. Berne, and G. L. Martyna, J. Chem. Phys. **97**, 1990 (1992).
[24] C. Braga and K. P. Travis, J. Chem. Phys. **123**, 134101 (2005).
[25] K. P. Travis and C. Braga, J. Chem. Phys. **128**, 014111 (2008).
[26] S. Toxvaerd, N. Larsen, and J. C. Dyre, J. Phys. Chem. C **115**, 12808 (2011).